Austenite stabilization from direct cementite conversion in low-alloy steels

Gregory N. Haidemenopoulos

Transformation induced plasticity (TRIP) effects associated with austenite dispersions in low alloy Fe-Mn-Si steels can be enhanced by austenite stabilisation. Austenite which forms during conventional intercritical annealing does not possess the required stability in order to exhibit TRIP effects. In this work, thermodynamic calculations indicated that it is feasible to form austenite by a cementite to austenite conversion which occurs under paraequilibrium conditions, i.e with partition of carbon but with no partition of substitutional alloying elements. In this way the austenite inherits the manganese content of cementite and is chemically stabilised. A treatment consisting of a two-step annealing has been examined. In the first step, soft annealing, an Mn-enriched cementite dispersion in ferrite is formed. In the second step, intercritical annealing, austenite nucleates on the cementite particles, which are consumed to form austenite. It was experimentally determined that this austenite has been enriched in manganese and carbon and, therefore, is stabilised. The conversion reaction is followed by the conventional austenite nucleation at ferrite grain boundaries. This austenite is lean in manganese and is not stable. The net effect of the two-step annealing treatment is a significant austenite stabilisation relative to simple intercritical annealing, indicating a potential for enhanced TRIP effects in this class of steels.

Austenitstabilisierung durch direkte Zementitumwandlung in niedriglegierten Stählen. Durch Umwandlung hervorgerufene Plastizitätseffekte (TRIP), die mit der Austenitverteilung in niedriglegierten Fe-Mn-Si Stählen zusammenhängen, können durch eine Austenitstabilisierung verstärkt werden. Austenit, der sich beim konventionellen Glühen im Zweiphasengebiet bildet, besitzt nicht die erforderliche Stabilität für TRIP-Effekte. Thermodynamische Berechnungen zeigen, daß sich Austenit unter Paragleichgewichtsbedingungen direkt aus Zementit bilden kann, d.h. unter Diffusion von Kohlenstoff aber ohne Diffusion von Substitutionslegierungselementen. Dadurch behält Austenit den erhöhten Mangangehalt des Zementits und wird stabilisiert. Eine zweistufige Glühbehandlung ist Gegenstand der Untersuchungen. In der ersten Stufe, beim Weichglühen, lagert sich Mn-angereicherter Zementit in Ferrit ein. In der zweiten Stufe, dem Glühen im Zweiphasengebiet, bilden sich Austenitkeime an den Zementitteilchen, die in Austenit umwandeln. Es wurde experimentell festgestellt, daß dieser Austenit mit Mangan und Kohlenstoff angereichert und dadurch stabilisiert ist. Dieser ersten Umwandlungsreaktion folgt die konventionelle Austenitkeimbildung an den Ferritkorngrenzen. Der so entstehende Austenit ist arm an Mn und instabil. Im Vergleich zum einstufigen Glühen im Zweiphasengebiet führt der zweistufige Prozeß zu einer wesentlichen Stabilisierung des Austenits. Hieraus läßt sich ein Potential zur Verstärkung der TRIP-Effekte in dieser Gruppe von Stählen ableiten.

Transformation induced plasticity (TRIP) associated with both bulk and dispersed austenite can give rise to remarkable mechanical behaviour in steels [1]. Enhancement of ductility and toughness associated with transformation induced plasticity has been reported in fully austenitic steels [2; 3] and in ultrahigh-strength steels containing metastable austenitic dispersions [4; 5]. Recently, it has been suggested to exploit the TRIP effect, associated with dispersed austenite, for the enhancement of ductility and formability in low alloy steels. Most work in this area has been performed on austenite stabilisation through the bainitic transformation. In a fundamental study, Tackechi and co-workers [6] found that intercritical annealing followed by bainite transformation produces significant quantities of retained austenite. Carbon enrichment and grain size refinement resulted in austenite stabilisation. The main effect of manganese was the reduction of the optimum cooling rate and the increase in the optimum bainite transformation temperature for stable retained austenite. On the other hand, the effect of silicon was to generally increase the stability of retained austenite. In a recent study [7] a strong correlation between uniform ductility and retained austenite stability has been attributed to TRIP effects in bainite-transformed low alloy steels.

Other techniques for austenite stabilisation have been exploited. Rao [8] demonstrated that excellent combination of strength and toughness can be obtained in low C-Mn steels which contain austenite particles distributed in a ferrite matrix. A three-step heat treatment was employed to produce the desired structure. In the first step the steel is fully austenitized and quenched to form lath martensite. In the second step the steel is heated below A_1 temperature to produce a mixture of ferrite and cementite. The third step involves intercritical annealing to produce a mixture of ferrite and austenite, followed by quenching. After quenching, some austenite is retained dispersed in a ferrite/martensite matrix. In Rao's work, this austenite had an acicular or lath-like morphology. It is believed that further improvements in ductility and formability can be obtained if the stability of dispersed austenite can be controlled for maximum transformation induced plasticity interactions at the stress state of interest for forming applications. In a recent work [9], the factors affecting the stability of dispersed austenite have been established. They include the austenite particle size, and chemical composition in stabilising solutes, the stress state and the strength of the matrix. The size dependence comes from the probability of finding a martensite nucleation site in the austenite particle, while the compositional dependence is due to the composition dependence of the thermodynamic driving force for martensitic transformation. The stress-state dependence comes from the interaction of the transformation volume change with stress triaxiality while the strength dependence comes from the mechanical contribution to the driving force for martensitic transformation. The stability of dispersed austenite was characterised by a single parameter, the M_s^σ temperature. A functional form has been developed in [9], linking the above-mentioned sta-

Assistant Professor Dr-Ing. Gregory N. Haidemenopoulos, Department of Mechanical and Industrial Engineering, University of Thessaly, Volos, Greece.

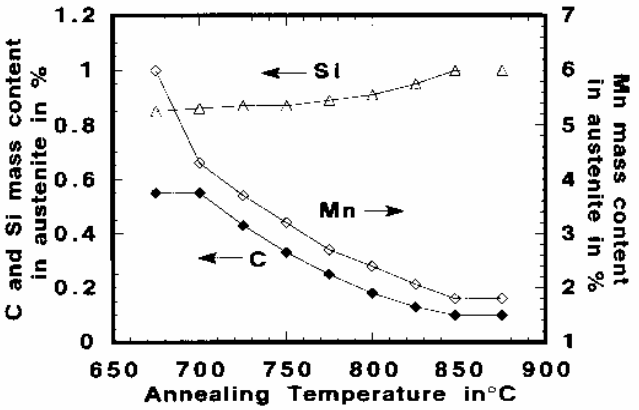

Figure 1. Calculated chemical composition (in C, Mn and Si mass contents) of austenite as a function of annealing temperature

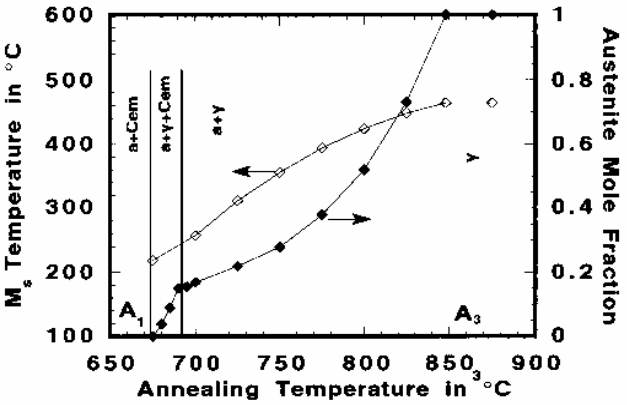

Figure 2. Calculated M_s temperature and mole fraction of austenite as a function of annealing temperature

bility parameters with M_s^σ temperature in Fe-Ni-Co steels. For maximum transformation induced plasticity interactions the M_s^σ temperature for the particular stress state of interest should be near room temperature. This, in turn, implies that the M_S temperature should usually be below ambient.

The aim of the present work is to further study austenite stabilisation by exploiting the cementite to austenite conversion during intercritical annealing. In case this reaction proceeds, then the austenite will inherit the Mn and C from the cementite and will be chemically stabilised. At the same time, by nucleating on the cementite, the austenite will assume the fine dispersion of the cementite. This will promote size stabilisation in addition to chemical stabilisation of the austenite.

These conditions can occur, however, only under thermodynamic paraequilibrium between cementite and austenite. Paraequilibrium is established between the two phases by the diffusion of carbon atoms only, while there is no diffusion of Mn atoms. Previous work in this area has been performed by Grujicic et al [10] who established the requirements for the conversion reaction by studying the thermodynamics of paraequilibrium cementite to austenite transformation in Fe-Mn-Si alloys.

In this work thermodynamic calculations were first performed to estimate the stability of austenite formed during conventional annealing, i.e equilibrium austenite. Then specific calculations were carried out to study the cementite to austenite transformation under paraequilibrium conditions, during intercritical annealing of ferrite/cementite mixture. Then experimental work is presented, which indicates that such a means of austenite stabilisation is possible.

Thermodynamic calculations

Equilibrium conditions. The thermodynamic calculations described here are aimed at assessing the stability (through M_S temperature) of the equilibrium austenite formed during intercritical annealing.

The calculations were carried out using Thermo-Calc computational thermodynamics program [11], for the chemical composition Fe-1.8Mn-1.0Si-0.10C (mass content in %). The equilibrium A_1 and A_3 temperatures were calculated to be 675 and 848°C, respectively. The chemical composition of equilibrium austenite formed between A_1 and A_3 is shown in **figure 1.** The austenite is depleted in stabilising solutes C and Mn as the annealing temperature increases, while there is a slight increase in Si. The data of figure 1 can be used for the calculation of the M_S temperature of the equilibrium austenite as a function of annealing temperature. For the calculation of the M_S temperature, Ishida's recent thermodynamic model [12] was adopted. This model takes into account magnetic and non-magnetic contributions to the chemical free energy and incorporates mechanical effects to the driving force for martensitic transformation. The resulting M_S temperature is shown as a function of annealing temperature through the two-phase ferrite/austenite and three phase ferrite/cementite/austenite regions in **figure 2.** In the same figure, the amount (in mole fraction) of the equilibrium austenite is also plotted. It can be seen that equilibrium austenite is not very stable since the M_S temperature varies between 220 and 460°C. Maximum stability of the equilibrium austenite is obtained at A_1 temperature for near zero mole fraction of austenite.

From the above calculations, it becomes obvious that other thermal treatments than simple intercritical annealing have to be developed in order to increase the stability of the precipitated austenite during intercritical annealing. Later, thermodynamic calculations are aimed at studying the paraequilibrium cementite to austenite transformation during intercritical annealing.

Paraequilibrium conditions. Soft annealing below A_1 temperature results in a two-phase ferrite/cementite structure, with the cementite finely dispersed in the ferrite matrix. Additionally the cementite is enriched in Mn. **Figure 3** shows the Mn mass content of cementite formed during the soft annealing treatment as a function of annealing temperature. It can be seen that soft annealing in the region of 650°C results in highly enriched cementite with Mn mass contents of approximately 17%.. If this high Mn content of cementite is inherited by austenite during intercritical annealing, it will certainly result in enhanced chemical stabilisation of austenite. In addition heterogeneous precipitation of austenite on cementite would ensure a sufficient grain size refinement of the austenite particles as well.

The cementite to austenite transformation has been studied in this work by assuming that paraequilibrium at

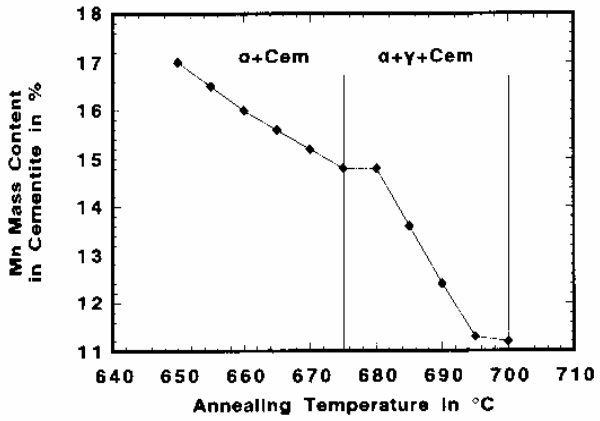

Figure 3. Calculated Mn content of cementite as a function of annealing temperature

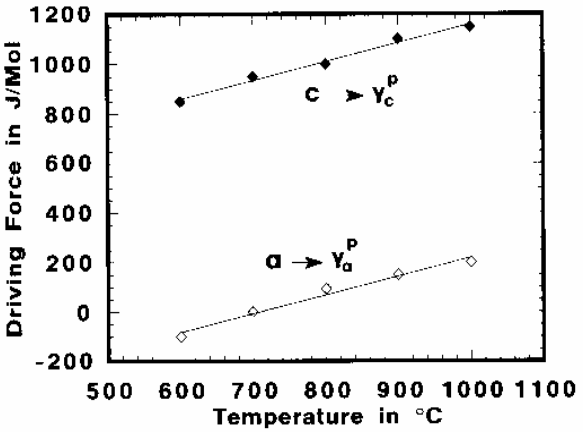

Figure 4. Calculated driving force (in J/mol) for the paraequilibrium formation of austenite from cementite (c --> γ_c^{ν}) and paraequilibrium formation of austenite from ferrite (α --> γ_α^{ν}) as a function of intercritical or supercritical annealing temperature

Table 1. List of symbols

M_s^d	temperature at which the required stress for martensitic transformation is equal to the yield stress of the parent phase
γ_c^p	austenite in paraequilibrium with cementite
γ_α^p	austenite in paraequilibrium with ferrite
T_{AUS}	austenitizing temperature
T_{SA}	soft annealing temperature
T_{IA}	intercritical annealing temperature

the cementite/austenite interface controls the transformation. In this case formation of austenite occurs by diffusion of carbon atoms only, while the Mn atoms do not diffuse.

In order to carry out the necessary calculations, the description of phases in the Thermo-Calc system has been modified by the introduction of a non-partitioning fictitious element M, which represents the non-partitioning elements Mn and Si. In this case new "paraequilibrium phases" for austenite, cementite and ferrite have been defined. The free energy of these phases is described in terms of M-based lattice stabilities and excess quantities. The latter are readily defined in terms of corresponding quantities for the non-partitioning elements Mn and Si included in the Thermo-Calc database. The procedure is described in detail in [13] and need not be repeated here.

The paraequilibrium phases defined are: α, ferrite in equilibrium with cementite at the soft annealing temperature; c, cementite which forms during the soft annealing treatment and having Mn content given in figure 3; γ_c^{ν}, austenite in paraequilibrium with cementite (c) and having the same Mn and Si content with cementite ; γ_α^{ν}, austenite in paraequilibrium with ferrite (α) and having the same Mn and Si contents with ferrite. For list of symbols see **table 1.**

At the intercritical annealing temperature, there will be a competition for the precipitation of γ_c^p or γ_α^p. The tendency for precipitation of the two phases can be estimated by calculating the corresponding driving forces for precipitation. The results of this calculation are shown in **figure 4.** It is evident that the driving force for the precipitation of γ_c^{ν} is higher than the driving force for the precipitation of γ_α^{ν} at all intercritical or supercritical annealing temperatures. After nucleation γ_c^{ν} grows into the cementite and converts it to austenite. During the conversion, carbon is rejected to the surrounding ferrite. The conversion reaction ceases when the carbon content in ferrite (α) becomes equal to that set by the c/γ_c^{ν} equilibrium [10]. Further growth of austenite requires the partition of Mn and Si, under local equilibrium conditions. The above results indicate that during intercritical annealing of a ferrite/cementite mixture, two types of austenite could form. Initially, γ_c^{ν} could form from direct conversion of cementite under the paraequilibrium conditions just described. This paraequilibrium austenite could, therefore, inherit the Mn content of cementite and be chemically stabilised. At the later stages of annealing the paraequilibrium reaction should cease and more austenite should form under local equilibrium by partitioning of Mn and Si. This austenite should be much leaner in Mn and, therefore, less stable than the paraequilibrium austenite γ_c^{ν}.

Therefore, soft annealing followed by short-time intercritical annealing seems to offer a stabilising potential for dispersed austenite, which is necessary for transformation induced plasticity interactions. This possibility has been investigated experimentally.

Experimental procedures

The chemical composition of the steel used in the present study is Fe-1.8Mn-1.0Si-0.12C (mass contents in %). The steel was produced as 50kg vacuum degassed ingot in 125mm x 125mm mould. After casting, the slab was machined to remove the as-cast surface, then hot rolled in a plate mill to 10mm thickness and subsequently cut into sections of 1m length. After milling on each side of the band to remove the decarburized layers, a final hot rolling operation in a 3-high mill reduced the thickness to 3.5mm. The steel was subsequently cold rolled to a final thickness of 0.8 mm.

The heat treatment schedule is shown in **figure 5.** T_{AUS} is the austenitizing temperature, T_{SA} is the soft annealing temperature while T_{IA} is the intercritical annealing temperature. Specimens 10mm wide and 50mm long were cut from the 0.8mm thick strips. The specimens were encapsulated in argon atmosphere and were austenitized at T_{AUS} = 900°C for 1 h, followed by water quenching. The specimens were then soft annealed at T_{SA} = 650°C for

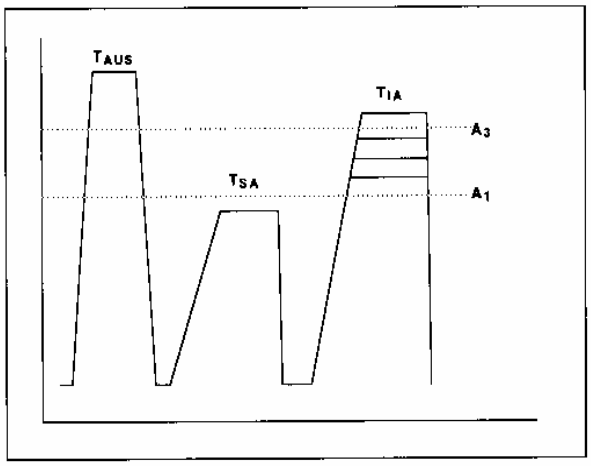

Figure 5. Heat treatment schedule for the formation of austenite via paraequilibrium conversion from cementite during intercritical annealing. T_{SA} is the soft annealing temperature and T_{IA} is the intercritical annealing temperature

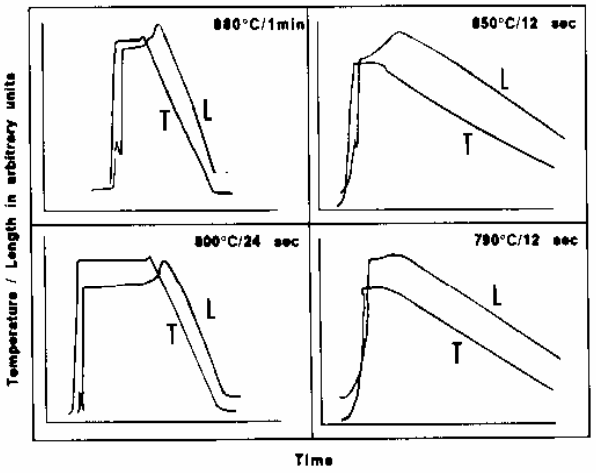

Figure 6. Temperature -time (T) and length - time (L) dilatometry data for four different annealing treatments

Table 2. Intercritical annealing treatments. T_{IA} is the intercritical annealing temperature while t_{IA} is the time at T_{IA}

T_{IA}, °C	t_{IA}, s
880	60
850	12
850	24
800	12
800	24
790	12
790	24

4min in a neutral salt bath and were then water quenched. Consequently, specimens of 10mm length and 3mm diameter were prepared in order to continue the heat treatment cycle in the dilatometer. Dilatometry was performed using an MMC dilatometer operating under vacuum. The specimen was supported between two platens. The heating was provided by two induction coils while the cooling was performed rapidly by the introduction of helium gas into

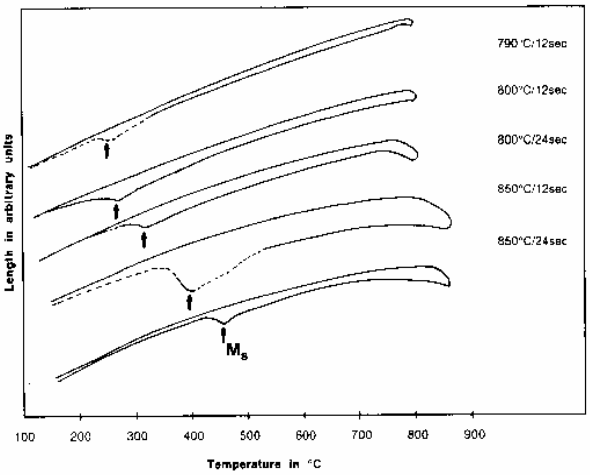

Figure 7. Length - temperature dilatometry data for five different annealing treatments. The arrows point to the respective M_S temperatures

the chamber. The heating rate employed was of the order of 500°C/min. All the intercritical annealing treatments were performed in the dilatometer in order to observe specimen length changes attributed to austenite formation and to determine the M_S temperature of the precipitated austenite. Following the soft annealing treatment, the intercritical annealing treatments performed in the dilatometer are shown in **table 2**. During dilatometry, the length vs time, temperature vs time as well as length vs temperature were recorded through the dilatometer computer control. The dilatometry specimens were subsequently sectioned for transmission electron microscopy (TEM). The specimens were sectioned with a slow speed diamond saw and were thinned to 5 µm thickness by 600 and 1000 grit emery papers.

Final thinning was performed in a twin-jet electropolisher at 12.5V. The solution used was 10% perchloric in methanol. During the process the solution was kept below -20°C. TEM was performed in a Hitachi H-700 TEM and a JEOL 100CX TEM. Electron energy loss spectroscopy (EELS) was performed in the Hitachi TEM which was equipped with an EELS detector.

Results

Combined temperature-time and length-time dilatometry traces are shown in **figure 6**. Immediately after the temperature is stabilised at the prescribed value and even before, there is a marked decrease in length indicating austenite formation. For the 880°C/60s treatment an initial abrupt length decrease is observed during the late stages of sample heating. After temperature stabilisation to the prescribed value (880°C) the length continues to decrease but at a slower rate. This behaviour indicates possibly two different mechanisms of austenite precipitation. During the cooling run, the spike on the length-time trace corresponds to martensitic transformation. This behaviour is similar in all treatments of table 1. Corresponding length-temperature plots from the dilatometric analysis are shown in **figure 7**. These plots conform with the behaviour described in figure 6 regarding austenite formation. In addi-

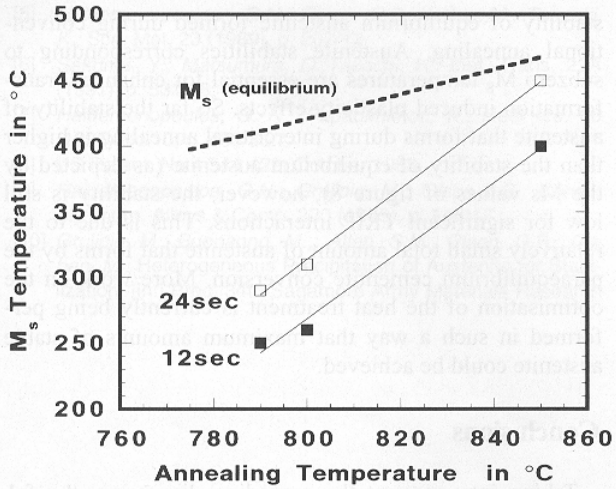

Figure 8. M_S temperature of austenite formed during intercritical annealing as a function of annealing temperature. The solid lines correspond to two different annealing times of 12 and 24 s, while the dotted line corresponds to the calculated M_S of equilibrium austenite

tion, the arrows indicate the corresponding M_S temperatures of the precipitated austenite during the intercritical annealing treatment. The measured M_S temperatures are plotted in **figure 8** as a function of annealing temperature together with the calculated M_S temperature of equilibrium austenite (dotted line) from figure 2 (Ishida model). The M_S is decreasing with annealing temperature, in agreement with model prediction. However, there is a marked difference in M_S values with the experimental M_S being lower than the theoretical prediction indicating higher stabilisation. The effect increases as the annealing temperature decreases.

Transmission electron microscopy was performed after soft annealing and on the dilatometry samples after intercritical annealing. A representative electron micrograph of the soft annealed structure is shown in **figure 9**. The micrograph indicates a dispersion of acicular cementite particles in a ferrite matrix. Average diameter of the cementite particles was estimated to be about 0.15µm. **Figure 10** shows a bright field (BF) image in (a) and the associated diffraction pattern in (b) of a dilatometry sample after intercritical annealing at 800°C/24s The BF image shows a particle containing internal twins. According to the dif-

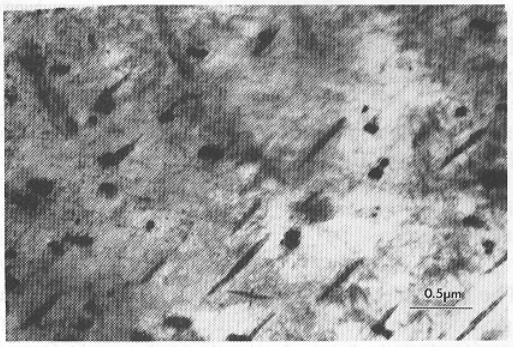

Figure 9. Transmission electron micrograph of the microstructure after soft annealing at 650°C for 4 min showing a fine dispersion of cementite particles in a ferritic matrix

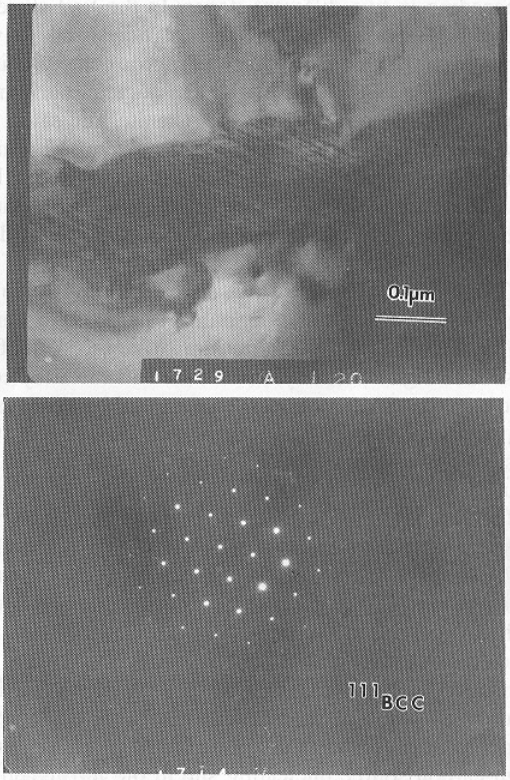

Figure 10. Bright field image (a) and associated selected area electron diffraction pattern (b) of a twinned martensite particle after intercritical annealing at 800°C for 24 s

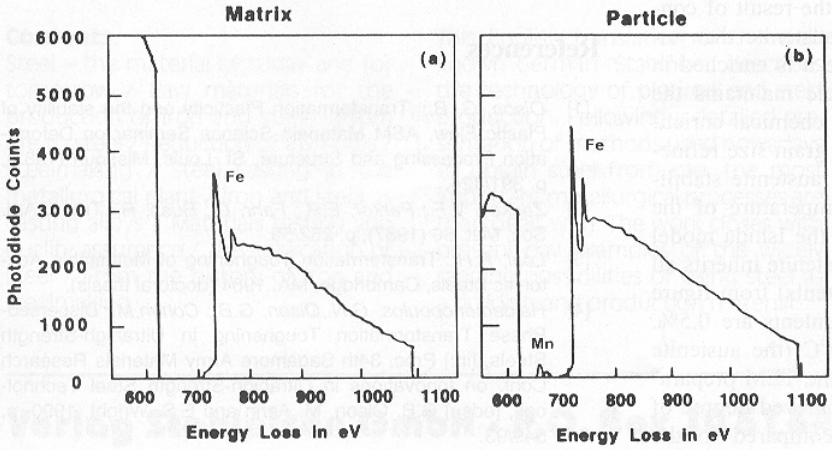

Figure 11. Electron energy loss spectra (EELS) of (a) the surrounding matrix and (b) martensite particle shown in figure 10, showing substantial enrichement of the particle in manganese

fraction pattern the particle was identified as [111] BCC, indicating that the particle is martensitic. **Figure 11** shows Electron Energy Loss Spectroscopy (EELS) spectra from the same particle and from the surrounding matrix. The spectra indicate a substantial Mn enrichment of the twinned martensitic particle.

Discussion

The dilatometric analysis indicated that during the late stages of heating to the intercritical annealing temperature, austenite starts to form. Austenite continues to form but at a different rate after the temperature has reached the specified annealing temperature. The different rates of austenite formation suggest that austenite precipitation is proceeding in two different stages. In the first stage, austenite nucleates at the cementite particles and grows by consuming the cementite. In other words cementite is converted to austenite according to the paraequilibrium reaction. In the second stage, the austenite nucleates at the ferrite grain boundaries according to the equilibrium α/γ-transformation which involves partition of the alloying elements. The paraequilibrium conversion is preceding the equilibrium austenite formation due to the higher driving force of the former , according to the calculations of figure 4. Therefore, due to the short annealing times employed, there will be a substantial amount of paraequilibrium austenite relative to the equilibrium austenite. The former possesses higher stability, since it inherits the alloy content of cementite. This argument is supported by the measured M_S temperatures in figure 8, which indicate substantial austenite stabilisation with respect to the formation of equilibrium austenite.

The results from TEM/EELS also indicate that cementite conversion to austenite is in fact taking place. The martensite particle of figure 10 is deformed by twinning. This means that the parent austenite particle had been enriched in carbon in excess of 0.4-0.5 (mass contents in %), since the lattice-invariant deformation of martensitic transformation of high carbon austenites is accommodated by internal twinning of the martensite phase [14]. The carbon enrichment of the austenite is attributed to nucleation on a high-carbon source nucleating site in the ferrite/cementite microstructure. In addition, the EELS spectra of figure 11 indicated significant enrichment of the particle in Mn. Both these experimental observations lead to the conclusion that the parent austenite particle is the result of conversion of cementite to austenite. The austenite then inherits the Mn content of cementite while it is enriched in carbon. In addition, the austenite particle maintains the small size of the cementite particle. The chemical enrichment (in Mn and C) in conjunction with grain size refinement of the austenite lead to substantial austenite stabilisation. A rough estimate of the M_S temperature of the austenite can be made by implementing the Ishida model [12]. The assumption is made that the austenite inherits all the Mn in cementite, i.e. 17% (mass contents) from figure 3 and that the austenite carbon mass contents are 0.5%. According to this calculation M_S = -10°C (the austenite particle transformed to martensite since the TEM preparation took place at below -20°C). The achieved degree of austenite stabilisation is substantially compared to the stability of equilibrium austenite formed during conventional annealing. Austenite stabilities corresponding to subzero M_S temperatures are essential for enhanced transformation induced plasticity effects. So far the stability of austenite that forms during intercritical annealing is higher than the stability of equilibrium austenite (as depicted by the Ms values of figure 8), however, the stability is still low for significant TRIP interactions. This is due to the relatively small total amount of austenite that forms by the paraequilibrium cementite conversion. More work on the optimisation of the heat treatment is currently being performed in such a way that maximum amounts of stable austenite could be achieved.

Conclusions

Taking into account the preceding discussion, the following conclusions can be drawn regarding the precipitation of austenite during intercritical annealing:

- austenite formation occurs in two stages; in the first stage, at short annealing times, austenite forms by a cementite to austenite conversion reaction while in the second stage austenite forms at the ferrite grain boundaries;
- the conversion of cementite to austenite occurs under conditions of paraequilibrium, i.e. partition of carbon but no partition of substitutional elements. This type of reaction is thermodynamically feasible (driving force considerations);
- the austenite which forms by the paraequilibrium cementite conversion inherits the high Mn and C contents of cementite and, therefore, is chemically stabilised;
- soft annealing below the A_1 temperature for the formation of an Mn-enriched cementite dispersion followed by short time intercritical annealing for the paraequilibrium cementite to austenite conversion seems to be a promising route for austenite stabilisation targeted for transformation induced plasticity applications.

Acknowledgements

The author is grateful to Prof. G.B. Olson and Dr. G. Ghosh of Northwestern University for useful discussions and for the kind help with dilatometry, TEM and EELS. This work has been partially supported by the European Commission through the project ECSC 7210-EC/702.

(A 01 123; received: 13. October 1995)

References

[1] *Olson, G. B.:* ,Transformation Plasticity and the stability of Plastic Flow, ASM Materials Science Seminar on Deformation Processing and Structure, St. Louis, Missouri (1982), p. 391/424.

[2] *Zackay, V.F.; Parker, E.R.; Fahr, D.; Bush, R.:* Trans. Am. Soc. Met. 60 (1967), p. 252/59.

[3] *Leal, R.H.:* Transformation Toughening of Metastable Austenitic Steels, Cambridge, MA, 1984 (doctoral thesis).

[4] *Haidemenopoulos, G.N.,Olson, G.B.; Cohen,M.:* Dispersed-Phase Transformation Toughening in Ultrahigh-Strength Steels, [in:] Proc. 34th Sagamore Army Materials Research Conf. on Innovations in Ultrahigh-Strength Steel Technology, [eds.:] G.B. Olson, M. Azrin and E.S. Wright, 1990, p. 549/93.

[5] *Haidemenopoulos , G.N.; Olson, G.B.; Cohen,M.; Tsuzaki, K.:* Scri. Met. 23 (1989), p. 207/12.

[6] *Sakuma, Y.; Matsumura, O.;Takechi, H.:* Met. Trans. 22A (1991), p. 531/38.

[7] *Haidemenopoulos, G. N.; Papadimitriou, K.:* steel res. 66 (1995) No.10, p. 433/38.

[8] US Patent, No.4 544 422, October 1985.

[9] *Haidemenopoulos, G.N.; Grujicic, M.; Olson,G.B.; Cohen, M.:* Journ. Alloys & Comp. 220 (1995), p. 142/47.

[10] *Grujicic, M.; Buonanno, M.,; Allen, S.M.; Olson, G.B.; Cohen, M.:* Heterogeneous Precipitation of Austenite for Stabilization, [in:] Proc. 34th Sagamore Army Materials Research Conf. on Innovations of Ultrahigh-Strength Steel Technology, [eds.:] G.B. Olson, M. Azrin and E.S. Wright, 1990, p. 527/47.

[11] *Sundman B, B. Jansson, B., Anderson, J-O.:* CALPHAD 9 (1985), p.153.

[12] *Ishida, K.:* Journ. Alloys & Comp. 220 (1995), p. 126/31.

[13] *Grujicic, M.; Haidemenopoulos, G.N.:* CALPHAD 12 (1988) No. 2, p. 187/92.

[14] *Cohen, M.; Wayman, C. M.:* [in:] Metallurgical Treatises [eds.:] J. K. Tien and J. F. Elliot, The Metallurgical Society of AIME, 1981, p. 445/68.